



HAL
open science

Scale-up of electrokinetic process for dredged sediments remediation

A. Benamar, M.T. Ammami, Y. Song, F. Portet-Kotalo

► **To cite this version:**

A. Benamar, M.T. Ammami, Y. Song, F. Portet-Kotalo. Scale-up of electrokinetic process for dredged sediments remediation. *Electrochimica Acta*, 2020, 352, pp.136488. 10.1016/j.electacta.2020.136488 . hal-02891088

HAL Id: hal-02891088

<https://normandie-univ.hal.science/hal-02891088>

Submitted on 3 Jun 2022

HAL is a multi-disciplinary open access archive for the deposit and dissemination of scientific research documents, whether they are published or not. The documents may come from teaching and research institutions in France or abroad, or from public or private research centers.

L'archive ouverte pluridisciplinaire **HAL**, est destinée au dépôt et à la diffusion de documents scientifiques de niveau recherche, publiés ou non, émanant des établissements d'enseignement et de recherche français ou étrangers, des laboratoires publics ou privés.



Distributed under a Creative Commons Attribution - NonCommercial 4.0 International License

Scale-up of electrokinetic process for dredged sediments remediation

A. Benamar^{a*}, M.T. Ammami^a, Y. Song^c, F. Portet-Koltalo^b

^aNormandie University, ULHN, LOMC UMR CNRS 6294, Le Havre, France

^bNormandie University, URN, COBRA UMR CNRS 6014, Evreux, France

^cInstitute of Ecology and Biodiversity, College of Life Sciences, Shandong University, Qingdao, 266237, China

*ahmed.benamar@univ-lehavre.fr

Abstract

Most of electrokinetic remediation (EKR) reported researchs were performed on small-scale laboratory devices and less field-scale studies are available in literature. Understanding the scaling-up process is essential for the application of the EKR at field scale. This paper presents the results of laboratory experiments performed at two scales (involving 0.4 kg and 40 kg of dredged sediment) to evaluate the potential of EKR process on both organic and inorganic contaminants, and the scaling-up effect. Mixtures of eco-friendly enhancing additives were used: a biodegradable chelating agent (citric acid) combined with a nonionic surfactant (Tween 20) were promising candidates for the simultaneous EK remediation of a multi-contaminated harbor sediment. The values of energy consumption from the large scale tests showed that efficient decrease of pollutant concentrations and sustainable remediation could be achieved with moderate energy costs. Obtained results also indicated that better removals of Cr, PAHs and PCBs were achieved with the large-scale device using less energy and additives. However, the distribution of the pollutants in the specimen after the EK remediation indicated that the electric field did not totally control the migration process and that the interaction with likely heterogeneity and inertial effects reduced the EK effectiveness at the large scale. This scaling-up investigation allows considering EK tests at a larger scale (field installation) with adjusted parameters from a small-scale investigation.

Key words: Electrokinetic Remediation, Scale-up, Sediment, Metals, PAHs, PCBs

1. Introduction

Management of dredged sediments is of great concern for maintaining harbor activities. In France, chemical guidance values are provided to assess the chemical hazard following the disposal of dredged sediment into environmental waters. Thus the restricted marine disposal of dredged sediment has led managers to manage ashore with a treatment to reduce their contamination level. Electrokinetic remediation (EKR) is a technology that has received attention as a practical *in-situ* and *ex-situ* remediation technique for low permeable clay-rich soil or fine-grained sediment. Many EKR studies aim to address the effectiveness of EK for the remediation of polluted soils and sediments and the operating conditions selected at laboratory-scale are generally the starting point for large-scale treatments [1–6]. The first investigations of EKR performed at laboratory-scale aimed to test heavy metal-spiked clays [7–14]. However, the obtained results from these studies could not be transposed for real multicontaminated sediments, because contaminants are much more mobile in spiked soils rather than in aged sediments. Researchers, therefore, started to test at laboratory-scale soils, sediments or wastes from contaminated sites [15–27]. Understanding contaminants behavior is more complicated when considering also lipophilic nonionic contaminants such as polycyclic aromatic hydrocarbons (PAHs) or polychlorinated biphenyls (PCBs). And far less studies than those considering only metals mention results about semi-pilot scale treatments of organics such as PAHs [28]. Most of the EKR experiments provided in literature are still dealing with small experimental devices and few on-site or large *ex-situ* installations have been developed in order to treat large amounts of sediments. So, in order to scale-up laboratory tests to field treatments, intermediate scale investigation appeared to be of a great interest [29,30]. Some papers have reported results for large-scale EKR [1,2,6,28,30,31] but there is a lack of reports regarding the scaling-up process. Gent et al. [1] compared lab-scale (a sample of 785 cm³) and pilot-scale field (64 m³ of material) tests for EK extraction of Cr

and Cd from contaminated soils. The process was found to be more efficient in the field since higher extraction rates were achieved at lower energy levels, as reported otherwise [32]. The lab-scale investigation conducted by Wieczorek et al. [2] allowed to design and scale-up a pilot plant for an *in-situ* test involving a soil volume of 12 m³, with an electric field strength and an electroosmotic flow comparable to the lab experiment. A field EKR of As⁻, Pb⁻, and Cu⁻ contaminated paddy soil was carried out in a real field on a pilot scale [31]. Lopez et al. [28] designed a pilot plant as an open system with two rows of three electrodes to study the EKR of a natural soil polluted with phenanthrene. The results showed that gravity and evaporation fluxes were more relevant than EK fluxes, and a low average removal was obtained. Villen-Guzman et al. [5,24] reported a research about convenient specific-energy requirements at different scales for three metals (Pb, Ca, Mg) removal, based in the amount of metal which could be actually mobilized, derived from fractionation analyses. Masi et al. [6] developed a two-dimensional reactive-transport model for the cost optimization of electrokinetic treatment of contaminated dredged sediments. The model was applied to an EKR prototype plant [23] treating 150 m³ of dredged sediments, and the model parameters were either calibrated using a lab-scale study (1.5 10⁻³ m³ of sediment) previously conducted for the same soil.

The complex nature of the field conditions (soil heterogeneity, unsaturated medium, large volume) and the inability to predict the field EK performance using selected laboratory operating parameters led to the unexpected efficiency in the field [2,3]. The transport processes (electroosmosis and electromigration) could also be affected by soil heterogeneity and climate conditions in the open field reactor. The control of electrolyte additives and pH remains the key features of the electrokinetic technology even at field scale. The electrode configurations used in many systems are generally simple, involving vertical electrodes in the polluted site, inserted into drilling wells or trenches around the area of concern. Experiments in terms of potential isoline density and homogeneity showed that a parallel linear

arrangement with an adequate spacing ratio between electrodes could be more favourable for on-site treatment [2]. But other EK processes involved the application of electric current to soil through a row of anodes surrounded by rows of cathodes [31]. Large scale *ex-situ* EKR devices were also developed using a rectangular tank that allows injecting additives solutions vertically or horizontally, avoiding the fluid losses and potential spread of contaminants beyond the treated area [4]. Based on the semi-pilot experiments (50 L), a project was conducted in South Korea [30] for *in-situ* application (area of 300 m²) using EK-solar cell remediation for a site contaminated with heavy metals (Cd, Cu, and Pb). The literature review of field EK experiments does not generally include the scale-up investigation between laboratory-scale tests and field facilities. Eventhough detailed characterization and investigations are carried out, many of the parameters for the design of *in-situ* EK treatment have to be arbitrarily set by the designers, because these parameters cannot be directly derived from preliminary data [6].

The present study reports a preliminary scale-up investigation to evaluate the potential of EKR process on pollutants removal from a real multi-contaminated dredged harbour sediment. The simultaneous removal of metals (Cd, Cr, Cu, Pb, Zn) and organic contaminants (PAHs and PCBs) were examined and the scaling-up effect was investigated. It involved two reactors at different scales and eco-friendly electrolyte additives were selected to enhance the organic and inorganic contaminants removal.

2. Conceptual considerations

In EKR processes, usually controlled parameters are mainly: voltage gradient, electrodes, reactor dimensions, material porosity, electrolyte additives. During EKR, various rate constants (linked to kinetics parameters), transfer coefficients (linked to equilibrium constants), transport properties (linked to fluid dynamics) and reactor dimension or electrodes configuration must be simultaneously taken into account to understand the complex processes

[4,6,31]. The most important part of any electrochemical technology is the electrochemical reactor, therefore the optimal design and scale-up plays an important role in the success of this technology. The transposition of optimized test parameters from laboratory-scale to a larger scale must follow many rules adapted from the similarity theory. The principle of similarity adopted involves dimensional analysis as a basic concept underlying the theory of transport processes and chemical reactors. So, various rate constants, transfer coefficients, transport properties and reactor dimensions must be combined in such a way that dimensional consistency is maintained [33]. The principle of scaling-up chemical process units requires the values of the corresponding dimensionless groups of the two units are similar. Several similarity criteria have been defined to guide engineers to scale-up a thermo-electrochemical reactor. The used criteria are those of geometric, kinematic, thermal and current/potential similarity between the two scales corresponding reactors:

- Geometric similarity is achieved by fixing the dimensional ratios of the corresponding reactors. But this criterion cannot be easily met, as increasing the length between electrodes would create a high voltage drop and a great energy consumption. Therefore, the geometric similarity is usually sacrificed in favor of current/potential similarity. Scale-up can also be achieved by using multiple cells and reactor units.
- Kinematic similarity is concerned with the fluid flow velocity within a system, mainly the electroosmotic flow (EOF) in simple EK system. So, it may be necessary to maintain similar flow velocity through the larger reactors.
- Thermal similarity includes matching the temperatures in corresponding portions of the reactors under comparison. This condition may be reached by temperature control through internal heat transfer surfaces, but it is difficult to maintain due to the effect of Joule heating particularly in large-scale systems.

- Current/potential similarity occurs between two electrochemical units when corresponding electrode potential and current density differences provide a constant ratio [33]. This is the most essential criterion in the scale-up concept because electrochemical reactors require electrical similarity, and requires a constant inter-electrode gap on scale-up. One factor used to quantify this similarity effect is the Wagner number (W_a) which is defined as:

$$W_a = \frac{k dV}{L dI} \quad (1)$$

where k is the electrolyte conductivity, V is the electrode potential, I is the current density and L is the characteristic length. For electrical similarity, the Wagner number in the two reactors should have the same value.

3. Materials and methods

3.1 Tested sediment characteristics

The studied marine dredged sediment was collected from a waterway of a harbor in Normandy (France). The sampling was performed using a bottom grab sampler from the sea-bottom surface layer (0–60 cm) at a water depth of about 5 m. The sediment samples, involving a very high water content (120%), were stored in sealed buckets and were left to settle for many days before which the supernatant was discarded, lowering the water content to a value close to 90%. The whole collected material was then homogenized and stored at 4°C. The physical and chemical properties of the sediment are presented in Table 1. pH value and electrical conductivity were measured according to the French NF ISO 10390 and NF ISO 11265 standards, respectively. Organic matter and carbonate contents were measured in accordance with the french NF EN 12879 and NF EN ISO 10693 standards, respectively. Particle size distribution was determined using a laser particle size analyzer (Multisizer 2000, Malvern Instruments, UK) according to the ISO 13320-1 standard. The water content and

hydraulic conductivity were measured according to NF EN ISO 17892-1 and NF X30-441 standards, respectively. The very low hydraulic conductivity was related to the large fine particles content (silt). The fine grained sediment involved also high organic matter and carbonate contents (so sediment pH was alkaline), which made this sediment interesting to study but likely difficult to remediate as regards to its high buffering capacity and its strong sorption capacity for lipophilic organic contaminants [34]. It must be also noted that the sediment redox potential was negative, because the reduced material was collected in-depth under a water column. The chemical analysis of the material indicated the multicontamination involving metals, polycyclic aromatic hydrocarbons (PAHs) and Polychlorinated biphenyls (PCBs) (Table 1). Only the 16 priority PAHs, as defined by US-EPA, and the 7 PCB indicators, as defined by the EU commission BCR, were measured. The analytical methodologies were described in a previous paper [35]. Briefly, samples were freeze-dried and crushed. Approximately 0.5 g sub-samples were digested into 8 mL of a nitric acid:hydrochloric acid 3:1 (v:v) mixture using microwave irradiation at 200°C for 4 min of ramping time and 4 min of holding time (Discover SP-D, CEM Corporation, Matthews, USA). The digested solutes were diluted in 25 mL water and filtered (0.45- μ m filter). Metal concentrations were analyzed using an ICP-AES system (ICAP 6300, ThermoFisher Scientific). Other sub-samples (5 g) were extracted by microwave-assisted extraction (MarsX, CEM Corporation) for PAHs and PCBs simultaneous analysis, using 40 mL of a toluene:acetone 1:1 (v:v) mixture at 130°C for 30 min (1,200 W). The extracts were filtered (0.2- μ m PTFE filters) and evaporated to 1.5 mL. Two internal standards (perdeuterated PAHs) were added, and then 1 μ L was injected (splitless mode, 285°C) into a gas chromatographer (6850 series, Agilent), coupled with a mass spectrometer (5975C). Separation was performed using a 60 mm \times 0.25 mm i.d. \times 0.25 μ m film ZB-5MS capillary column from Phenomenex, with helium as a carrier gas (1.4 mL min⁻¹). The oven temperature

was programmed at 60°C for 1.2 min, increased to 190°C (40°C min⁻¹) and then to 305°C (6°C min⁻¹). The detector operated at 70 eV in electron ionization mode. Quantification was based on selected ion monitoring for better sensitivity.

Table 1: summary of physical and chemical characteristics of the tested sediment

Parameters	Values
Particles < 2 µm (clays) (%)	5.9 ± 1.7
Particles from 2 to 63 µm (silts) (%)	75.1 ± 1.6
Particles from 63 to 2000 µm (sand) (%)	18.9 ± 3.3
Organic matter content (%)	11
Carbonate content (%)	30
Hydraulic conductivity (m/s)	<10 ⁻⁷
pH (n=3)	8.3 ± 0.1
Electrical conductivity (µS/cm) (n=3)	2200 ± 80
Redox potential (mV) (n=3)	-76 ± 8
∑ ₁₆ PAHs (priority) (mg/kg DW) (n=5)	2.114 ± 0.063
∑ ₇ PCB (indicators) (mg/kg DW) (n=5)	0.192 ± 0.014
Metals (mg/kg DW) (n=5)	410.51 ± 21.29
Cd (mg/kg DW)	4.02 ± 0.05
Cr (mg/kg DW)	136.68 ± 18.58
Cu (mg/kg DW)	39.21 ± 0.06
Pb (mg/kg DW)	59.88 ± 0.58
Zn (mg/kg DW)	170.72 ± 2.02

3.2. EK set up and test procedure

Two different devices were designed as reactors for EKR of the dredged sediment: a small cylindrical cell (Fig. 1a) and a large tank (Fig.1b). The small cell (4.9 cm inner diameter \times 19.2 cm length L), described in previous papers [22,36], involved three compartments: two electrode reservoirs (5 cm-L) and a central compartment (14.2 cm-L) filled with the sediment to be treated. Two graphite electrode plates (10 cm-L \times 2.5 cm-H \times 0.5 cm-W) were placed in each electrode compartment, which were separated from the sediment by perforated grids and porous fiber glass papers (0.45 μ m). Two pumps were filling each electrode reservoir with aqueous solutions with a low flow-rate (10 mL h⁻¹). The large device was built as a rectangular box made of polyvinyl chloride with internal sizes of 80 cm (L) \times 20 cm (W) \times 25 cm (H). It consisted of three compartments separated by grids and filters (0.45 μ m): two electrode compartments (10 cm-L) and a sediment chamber (60 cm-L). The sediment volume (20 \times 20 cm² cross section) involved was approximately 100 times greater than that of the cylindrical cell. Two tanks (5 L) contained the electrolyte solutions which were pumped to the electrode compartments using two peristaltic pumps (03S STEPDOS-KNF-Lab) at a flow rate of 50 mL h⁻¹. Two graphite electrode plates (20 cm-L \times 10 cm-H \times 1 cm-W) were inserted into the electrode compartments. Three horizontal plates covered the device to limit evaporation.

Mixtures of eco-friendly enhancing additives for the treatment of the multi-contaminated harbor sediment were used, according to the results of the previous research [36]. The additives involved 5 g L⁻¹ Tween 20 (TW20) as anolyte and 5 g L⁻¹ Tween 20 + 0,1 mol L⁻¹ citric acid (CA) as catholyte. Briefly, it was demonstrated that the addition of a nonionic surfactant in electrolytes was more favourable for the simultaneous removal of metals and PAHs than an anionic one; moreover the synthetic Tween20, used ten times above its critical micelle concentration, appeared to be non toxic in bioassay tests after EK treatments [35]. Citric acid (CA) was only added in catholytes to avoid sediment alkalisation (inherent to EK

process) at the cathode side; it was used at 0.1 M, which was enough to significantly enhance electroosmotic flow and metal removal without any toxicity effect. The controlled parameters of the electrochemical process were mainly the voltage gradient, the shape and the installation of the electrodes, the reactor dimensions, the sediment porosity and the enhancing additives flow rate. Before designing the large-scale reactor, considerations of which electrochemical parameter to keep constant were made. In a previous test in the large reactor the use of the same voltage gradient (1 V cm^{-1}) as in small reactor induced material heating and shrinkage. So, in this large-scale test, voltage gradient was kept close to 0.5 V cm^{-1} and in both reactors, plate graphite electrodes were used and the system was closed. The pulse voltage gradient was applied in both reactors by alternating 5 days-on and 2 days-off voltage. Alternating voltage could re-equilibrate the chemical balance at the solid-liquid interface during the rest phase and could favor the desorption of contaminants from solid particles, as reported in previous studies using similar materials [25]. The selected test parameters for scale-up are summarized in Table 2. In this first approach of scale-up the sediment temperature in the two reactors was maintained as similar as possible, around 20°C . Most of the parameters were adjusted in order to achieve similar current density, which is the most important similarity factor to keep.

At the end of each test, the sediment was extracted and sliced. The small-cell sample was cut into four 3.5 cm-L slices (Fig. 1a) which were air-dried and submitted to physicochemical analysis (contaminants concentration, pH and EC). EK post-run soil from the large box were sliced into forty-eight (from up- and down-layers), $10 \text{ cm} \times 10 \text{ cm} \times 5 \text{ cm}$ sections (Fig. 1b) with a stainless steel knife. Each section was weighed, homogeneized and stored in disposable bags at 4°C until further analysis of metals, PAHs and PCBs (see section 3.1). Prior to analysis, pH, moistures and EC were also determined for each sediment section.

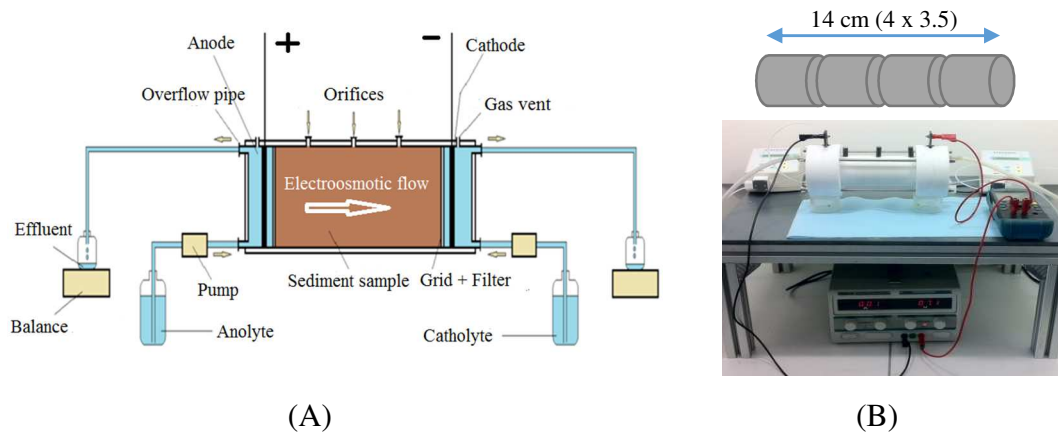


Figure 1a. Schematic diagram of the experimental setup of the small EK reactor (A) with cutting of the sediment slices and device view (B)

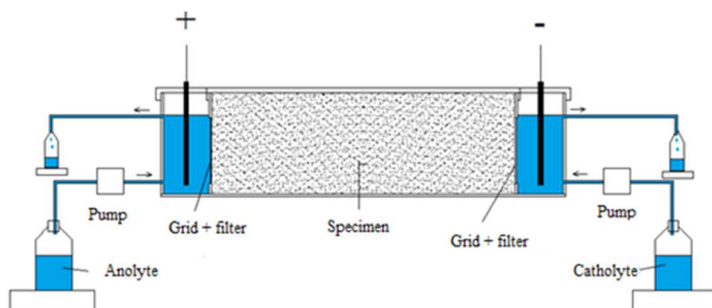
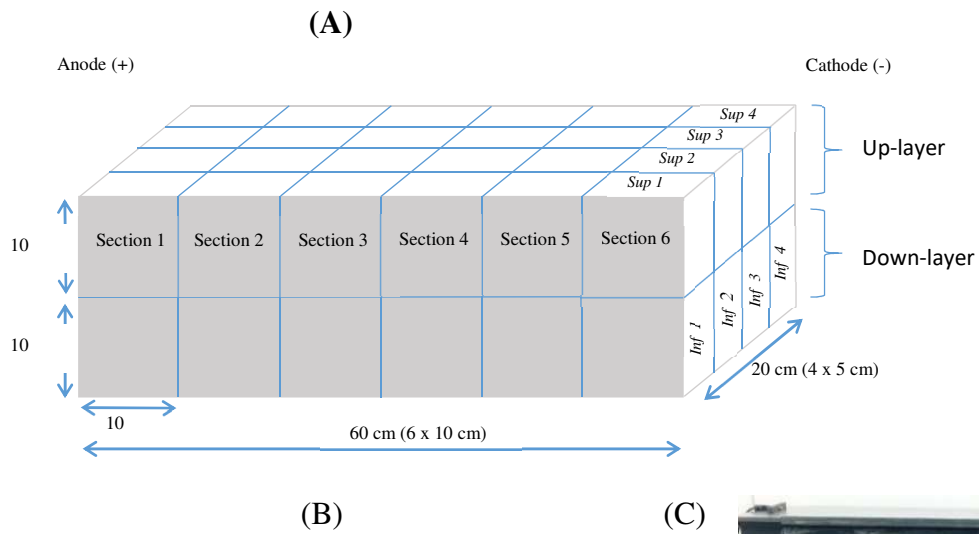


Figure 1b. Schematic diagram of the experimental setup of the large EK reactor (A) with cutting of the sediment slices (B) and device view (C)

Table 2. Operating parameters in the two EK reactors

Parameters	Small reactor (S)	Large reactor (L)	Ratio (L/S)
Anolyte	Tween 20 (5 g/ L)		
Catholyte	Tween 20 (5 g/ L) + citric acid (0.1 mol/L)		
Electrodes gap (m)	0.14	0.60	4.3
Sediment volume (L)	0.28	24	85
Voltage gradient (V cm ⁻¹)	1	0.5	0.5
Additives flow rate (mL h ⁻¹)	5	50	10
Average current density (A m ⁻²)	5	7.5	1.5
Duration of EK treatment (d)	21	56	2.7

4. Results and discussion

4.1. Variation of electric and chemical parameters

Figure 2 shows the evolution of current density during the EK treatments in the small and large reactors. The global trend of electric current density displayed in the two cases a high value at the beginning of the test before a drastic decrease, in particular after each restart of the on-voltage period. The current density magnitude overall decreased along successive on-voltage cycles before reaching stable values. The high current density value which rised at the EK process start, was ten times greater for the large reactor, and decreased faster for the small reactor. So, the average value of current density (Table 2) remained in the same order of magnitude in the two reactors. The alternate nature of the applied voltage led to the reactivation of the current at each cycle but its amplitude decreased with time owing to the decrease of available free ions. The current density decreased less rapidly in the large reactor, indicating that, after an important depletion during the on-voltage cycle, the restoration of the ions content after two days 'off' was more important because larger ions amounts were

available [36]. Opposite to the small reactor, the current density value (Table 2) remained important (1.5 times higher) despite the process was longer at the large scale. The measured initial values of electric conductivity (EC) were 2.30 mS cm^{-1} and 1.17 mS cm^{-1} in the small reactor and the large one, respectively. At the end of each EK test, this parameter reached the highest values of 4 mS cm^{-1} and 0.62 mS cm^{-1} at the anode side, and only 0.5 mS cm^{-1} and 0.17 mS cm^{-1} in the central specimen sections closest to the cathode side, in the small and large reactor, respectively. The spatial distribution of EC (Fig. 3), measured at the end of the test in the large reactor showed higher recorded data near the anode where ions concentrated mainly, but the magnitude of this parameter was drastically decreased compared to the initial value (Fig. 3). In the two reactors, an heterogeneous distribution was recorded between the electrode sides and the middle specimen; the central sections closest to the cathode side were the most depleted in ionic species. Besides, in the case of the large reactor, electrical conductivity measurements provided slightly higher values in the up-layer of the large reactor, with mean values of $0.54 \pm 0.21 \text{ mS cm}^{-1}$ and $0.45 \pm 0.25 \text{ mS cm}^{-1}$ for the upper and down layers, respectively. This statistically non-significant difference ($p\text{-value} > 0.05$), eventhough low, was corroborated by lower pH values recorded in the up-layer. Indeed, the mean pH value in the uppe layer was 7.08 ± 0.27 , compared to 7.30 ± 0.28 in the down layer (Fig. 4), providing a difference which was statistically non-significant ($p\text{-value} > 0.05$) but showed that the upper layer was a little more acidified than the bottom one and that the probability of finding more soluble metal ions (electric conductors) was higher. In fact, the bottom sediment layer appeared to be more compact at the end of the large EK test; it contained less water: $92.3 \pm 15.0\%$ in average, compared to $101.4 \pm 14.7\%$ in the upper layer. Even if the difference was not statistically significant ($p\text{-value} > 0.05$), this tendency led probably to a poorer transport of soluble species in the dryer down sections.

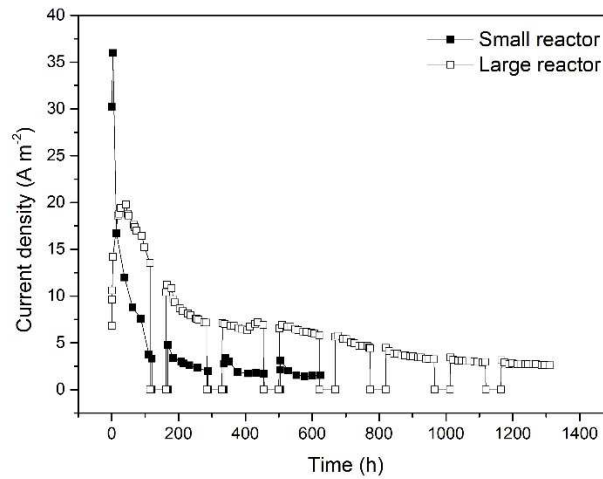


Figure 2. Evolution of electric current density during EK treatment in a) the small reactor, b) the large reactor

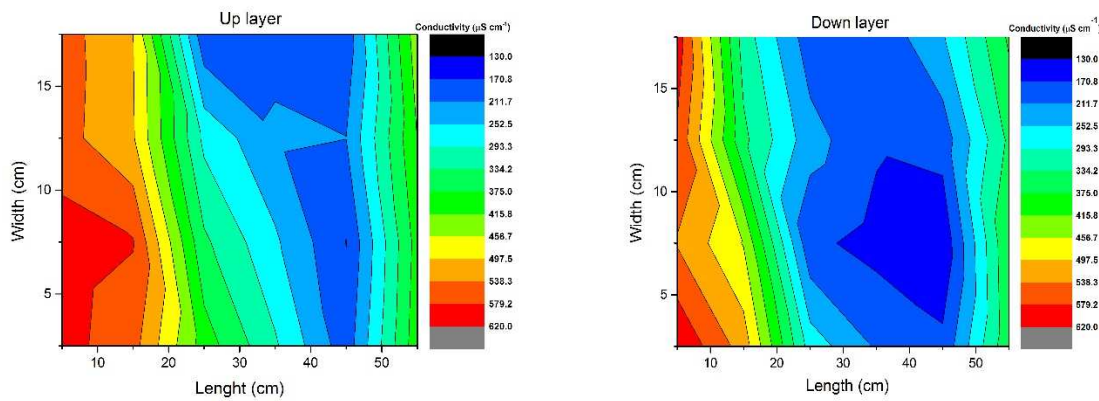


Figure 3. Spatial distribution of electrical conductivity of sediment in the large reactor after the EK test in a) up-layer and b) down-layer

According to Eq. 1, the evaluation of the Wagner number W_a provided mean values close to 0.4 and 0.6 in the small and large reactors, respectively. These values were averaged for all the sub-samples (from the anode to the cathode and for up- and down-layers) and for all the duration of the test and provided a quite good similarity. In addition, if reducing the comparison to electrical parameters only, electrical similarity can exist between two compared units when the corresponding electrode potential and current density differences

provide a constant ratio [33]. From Table 2, this ratio (dV/dI) was close to 2.8 and 3.0 $\Omega \text{ m}^{-2}$ in the small reactor and the large one, respectively. These values are close, concluding that electrical similarity was respected.

The energy consumption in EK systems is a criterion which determines the sustainability of the technology when applied in the field facility. The average power consumption was evaluated to 0.095 W (340 W/m³ of wet material) and 7.280 W (303 W/m³ of wet material) for the small and large reactors, respectively. The electric power values developed in the two reactors per unit volume of treated material were quite similar. However the energy consumption per unit volume expended in the large reactor (407 kWh/m³) was more than twice higher than in the small reactor (171 kWh/m³) because of the longer duration of the EK treatment.

The results of measured pH showed the development and advance of the acid front from the anode towards the cathode (Fig. 4). For the two EK treatments, adding CA in the catholyte avoided the alkalisation (due to water electrolysis) of the sediment sections near the cathode side but the effect of CA was less pronounced at the large scale: pH was decreased from 8.3 to 7.7-7.8 in the sections near the cathode side for the small-scale treatment whereas it was only maintained around 7.8-8.4 in the sections near the cathode side for the large-scale treatment (Fig. 4). Due to the large volume of sediment and its high buffering capacity, sediment acidification was limited at the anode side of the large reactor. Overall, the pH values in the various sections of the large reactor were not low enough to solubilize the ETs in significant amounts. As noted previously, the pH values in the up-layer of the sediment were slightly lower than those in the down-layer. The sediment near the anode side was more acidified (due to water electrolysis) in the small reactor (pH=6.5) than in the large one (pH=6.8-7.4) (Fig. 4), which could explain the higher values of EC at the anode side

in the small reactor. The high buffering effect which was detrimental for the acidification of the sediment specimen, was not favourable for metal solubilisation.

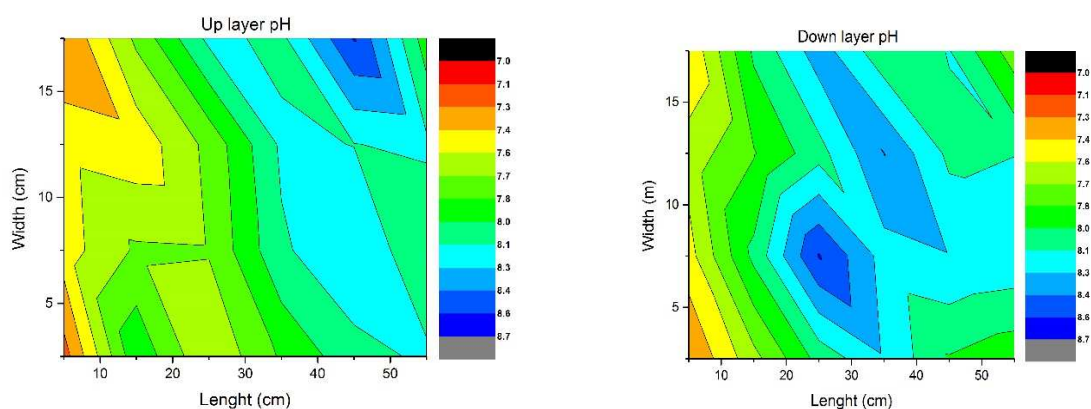


Figure 4. Spatial distribution of pH of sediment in the large reactor after the EK test in up-layer (left) and down-layer (right)

4.2. Variation of the electroosmotic flow (EOF)

The results from Fig. 5 indicated that in the small-scale reactor, the main EOF was directed from the anode to the cathode, while in the large scale reactor the EOF occurred towards the two electrodes and was more activated by the higher current density. The amount of transported fluid was higher towards the cathode but if the volume recovered at the anode side was not so important, the slope of the cumulated EOF at the anode side indicated that the reverse direction of EOF was rising, owing to the modification of chemical conditions. The average value of EOF obtained in the large-scale test (6 mL h^{-1}) was 30 times higher than that measured from the small-scale device (0.2 mL h^{-1}), owing to the greater flow rate of electrolyte supply which was ten times higher in the large reactor than in the small one (Table 2). The corresponding flow velocities ($4 \cdot 10^{-8} \text{ m s}^{-1}$ and $3 \cdot 10^{-8} \text{ m s}^{-1}$ in the small and large reactor, respectively) indicated that the kinematic similarity was reached. It is possible that the more important electrolyte supply contributed to a better penetration of CA throughout the

sediment specimen in the large reactor, generating the higher EOF, particularly from the cathode to the anode side. It is a known effect of CA which induces high EOF values compared to other strong acids [20]. Moreover, in the 6.8-8.4 pH range, CA was in its anionic form, leading to its electromigration and concentration towards the anode side.

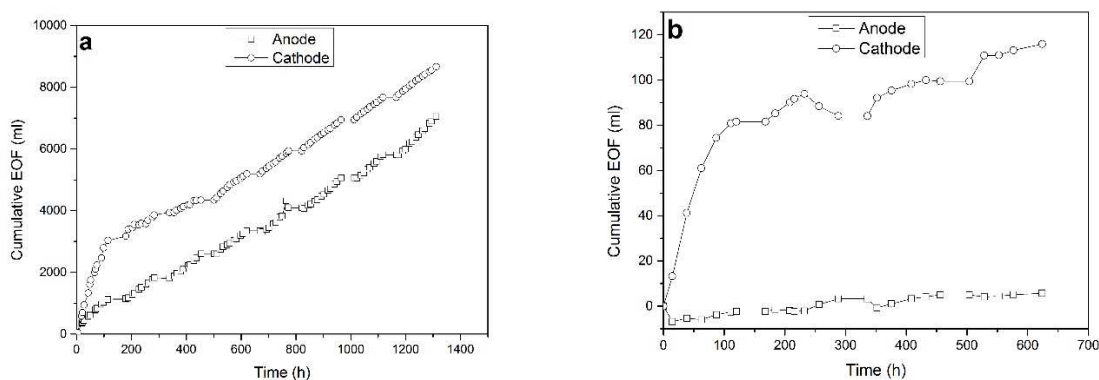


Figure 5. Variation of the cumulated electroosmotic flow (EOF) during EK treatments in a) the small and, b) the large reactor

The previous results were discussed in order to understand how EK processes can contribute to pollutants' removal. The objective of scale-up was to adapt laboratory operating parameters (following similarity between electrochemical parameters) to reach if possible similar removal results in field or at semi-pilot-scale. This objective cannot be easily reached if any compartment of the large reactor present local conditions hindering EK process efficiency.

4.3. Contaminants removal

The results of contaminants removal (Table 3) indicated that the large reactor could provide better removal of many metals (especially Cr and Pb) and PAHs. The additives used in these tests helped to remove the less strongly sorbed PAHs and PCBs. The harbour sediment was particularly rich in organic matter (Table 1), which strongly sorbed lipophilic PAHs and PCBs. Despite this severe constraint, the nonionic Tween20 surfactant contributed

to desorb and solubilize the lipophilic organic compounds. But to migrate, the organic pollutants included inside the neutral micelles necessitate a sufficient EOF. It was the case for the large reactor, where a high EOF allowed PAH migration to the electrode compartments. But in the case of the small reactor, EOF was not sufficient to allow PAH removal. The PAHs concentration measured after the large-scale treatment (Fig. 6) provided an heterogeneous distribution showing (i) a better removal near the electrodes, as EOF was strong from the anode to the cathode but also in the reverse direction, (ii) the accumulation of pollutants in local zones of the large reactor and (iii) the better transport of species towards the upper and less dry layer (Fig. 6 a and 6 b). Concerning PCBs, the mean removal results were similar for the two reactors (Table 3). It seems that PCBs migration did not depend only on EOF strength, unlike PAHs. It is possible that PCBs, which own a dipole moment (unlike PAHs), could also migrate through the influence of the electrostatic attraction in the electric field. In the case of the small reactor, PCBs were better removed near the electrode sides, and more particularly near the cathode side. In the case of the large reactor, Fig. 6 c and 6 d indicated great heterogeneities in the horizontal and vertical directions. As for PAHs, the dryer bottom layer, particularly in the middle of the sediment, concentrated more PCBs. The great inter electrodes gap in the large scale may lead to potential drop, affecting the electric field within the specimen, reducing the horizontal transfer ability of the species

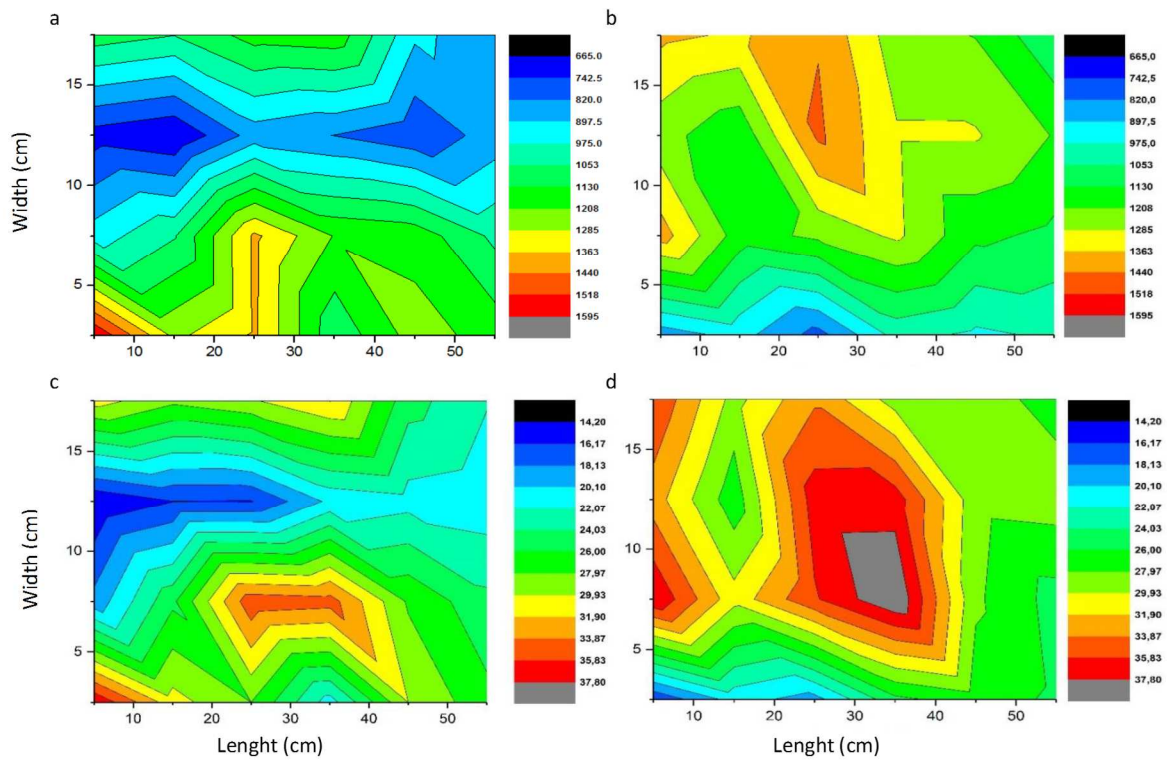


Figure 6: Spatial distribution of the concentrations of the Σ_{16} PAHs and the Σ_7 PCBs ($\mu\text{g kg}^{-1}$) in the large scale specimen after the EK test (length measured from the anode to the cathode) a: PAHs in the upper layer, b: PAHs in the down layer, c: PCBs in the upper layer, d: PCBs in the down layer

Except Cr, metal removals remained low with the used electrolyte additives (Table 3). Overall, higher removals were obtained in the large-scale reactor compared to the small-scale, indicating that the promising results obtained in other laboratory small-scale experiments [12, 20, 25, 34, 36], using different additives, might have the potential to be scaled-up without deteriorating the removal results for each pollutant group.

Table 3. Contaminants removal from the two different scale reactors

Contaminant removals (%)	Small reactor	Large reactor
Cd	4,5 ± 0,8	0
Cr	3,1 ± 1,8	22,7 ± 1,2
Cu	0	5,3 ± 2,4
Pb	3,5 ± 0,7	9,5 ± 1,4
Zn	2,3 ± 0,9	0
∑ ₁₆ HAPs	0	20,5 ± 7,6
∑ ₇ PCBs	22,8 ± 3,7	21,5 ± 8,1

As mentioned previously, the dredged harbor sediment was very rich in carbonates, which hindered the acidification of the sediment. So at $6.5 < \text{pH} < 8.4$, the free cations of the metals were insignificant and metal hydroxides, which precipitate, were a majority. However, the presence of CA, in the citrate form (CA^{3-}) in this pH range, could lead to the formation of soluble citrate complexes. For Pb, Cd, Cu and Zn, 1:1 complexes $[\text{M}_{\text{II}}(\text{CA}^{3-})]^{-}$ were more stable while for Cr, the dimeric complex $[\text{Cr}_{\text{III}}(\text{CA})_2^{3-}]^{4-}$ could be more stable [20,36]. The charge of the dimeric complex with Cr and the higher current density in the large reactor could explain why Cr was better removed through electromigration to the anode side in the large EK test. Also, $[\text{Pb}_{\text{II}}(\text{CA}^{3-})]^{-}$ is a more stable complex than $[\text{Cd}_{\text{II}}(\text{CA}^{3-})]^{-}$ which could explain why Pb better migrated to the anode side. The stability constants of $[\text{Cu}_{\text{II}}(\text{CA}^{3-})]^{-}$ and $[\text{Zn}_{\text{II}}(\text{CA}^{3-})]^{-}$ could also probably explain their removal results. But in general, only the quite mobile metals could be complexed and solubilized. Indeed, the sediment was rich in reduced species, as its redox potential was negative (Table 1), which probably contributed to form immobile metal complexes with sulphur-containing species. The mineralogical speciation of the sediment might have confirm the presence of these refractory mineral fractions where metals are strongly sorbed even at $\text{pH} < 3$.

Metals concentration measured after the large scale treatment provided various distributions showing (i) metal depletion, particularly in the central sections, for Cr and Pb (Fig. 7). An accumulation of these metals near the anode side showed that the migration towards this electrode was not finished when the EK test was stopped. So it could have been interesting to increase the duration of this test; and (ii) there was an accumulation of metals (Cd, Cu) in local zones of the large reactor which contributed to their low removal. Similar results were reported in literature [6] where the modelisation showed the faster advance of the acidic front from the anode to the cathode along the anode-cathode axis. It was attributed to the higher electric field strength in this region than at the borders of the domain. As a result, residual Pb concentration followed the same trend and higher transport rates were observed along the anode- cathode line, leading to the accumulation of Pb in a narrow zone of the domain. These accumulation areas formed dead zones from where the contaminant could be hardly removed, especially in the upper and lower corners. To optimize removal in the corners of the reactor, the anode-anode distance must be carefully evaluated and properly chosen as a function of the target removal requirements [6]. These results demonstrated that heterogeneities in sediment at large scale are difficult to predict at small scale.

The vertical parallel configuration of electrodes has been widely applied in EKR because it provides a direct and efficient electric field for horizontal ionic migration. However when using large scale EK devices including a large volume of sediments, the contaminants could also migrate upward or downward along with the liquid through dispersion and diffusion, although they mainly migrate according to the horizontal electric field [1,6]. The spatial distribution of Cr and Pb in the sediment of the large reactor (Fig. 7) showed that metals were less concentrated in the down-layer. Overall, metals migrated mainly towards the anode side but this migration was more effective within the down-layer. It is possible that the higher concentration in the up-layer could be due to the migration of ions from the down to

the up-layer. The higher moisture measured in the up-layer could suggest that sediment settlement contributed to transfer more important fluid (and the contained metal fraction) concentration in that side. The investigation conducted on a field pilot-scale [1] resulted also in a better removal efficiency of chromium and cadmium in comparison to laboratory results. This indicated that there was less electrical resistance in the field facility compared to laboratory tests. The same conclusion can be sustained in this study from the sediment resistivity values in the large reactor ($7 \Omega\text{m}$) and the small one ($20 \Omega\text{m}$).

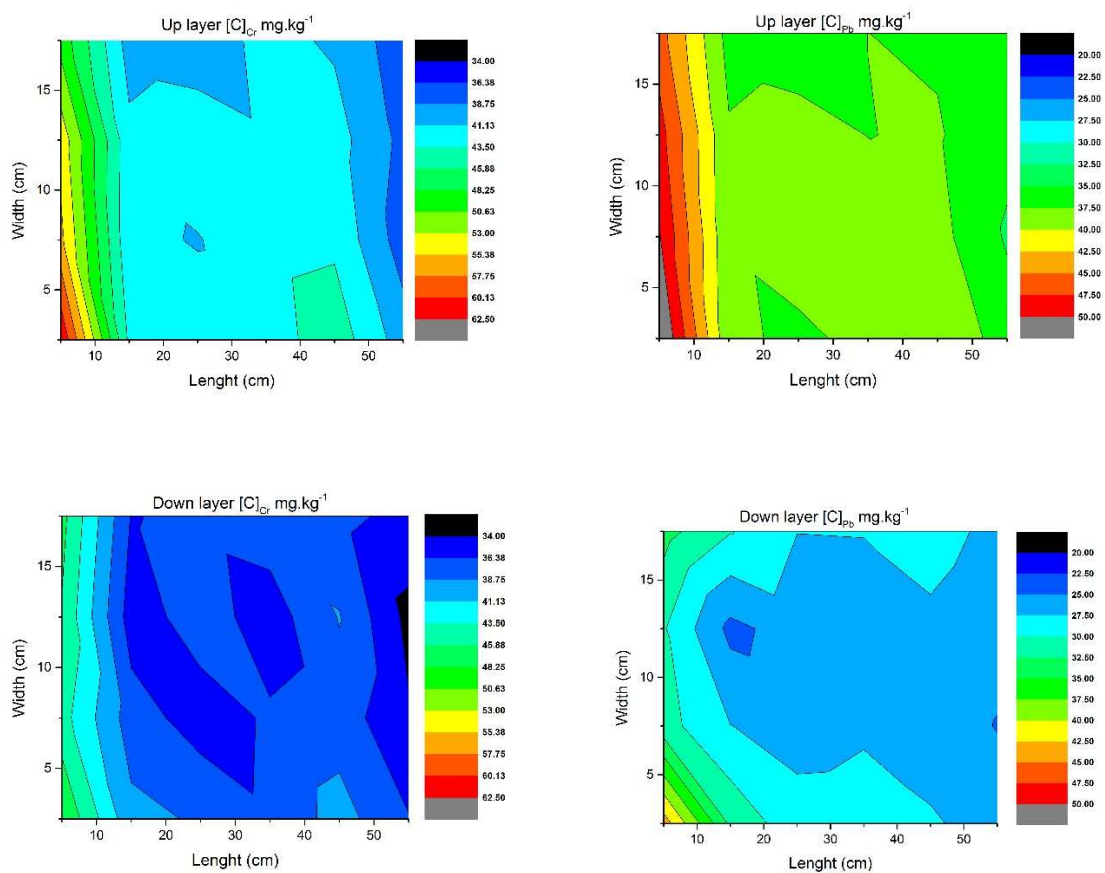


Figure 7. Spatial distribution of Cr and Pb (mg kg^{-1}) concentrations in the large scale specimen after the EK test (length measured from the anode to the cathode) a: Cr in the upper layer, b: Pb in the upper layer, c: Cr in the bottom layer, d: Pb in the bottom layer

5. Conclusions

Among literature, most EK investigations are performed at a small lab scale and this study investigated how to adjust electrochemical parameters to scale-up the EK process from a small reactor to a large one without affecting the efficiency process. Scale-up of EKR requires the adaptation of electrochemical parameters and in this study, the electrical and kinematic similarities were applied through voltage/current density (Wagner number) and flow velocity between the two scales. The mixture of a chelating agent (citric acid) and a nonionic surfactant (Tween 20) proved to be a promising combination for EK multi-decontamination of metals and PAHs/PCBs from a particularly refractory real harbour sediment, which presented high amounts of carbonates, organic matter and strongly sorptive reduced species. The results of pollutants removal showed the better effectiveness of EKR at the larger scale, even though removals obtained at the small scale were low. The distribution of the pollutants in the large reactor after the EK test indicated that the electric field did not totally control the migration process and the interaction with heterogeneity and inertial effects reduced the EK effectiveness at the large-scale.

The values of energy consumption from the large-scale tests showed that efficient pollutants concentration decrease and sustainable remediation could be achieved with a moderate energy cost. However, even though removal was better in the large-scale test, optimization is still necessary, especially for the electrodes gap and additives supply. Longer treatment was needed for the large scale remediation where strong heterogeneities could arise. If EK process must be actually tested at a small-scale in a preliminary step, it must be rapidly extended to a larger (semi-pilot) scale with similar dimensionless parameters. It seems essential to adjust properly operating parameters required for larger modular systems, and then the process might be extended to the field scale with better economical effectiveness.

References

- [1] D.B. Gent, R.M. Bricka, A.N. Alshawabkeh, S.L. Larson, G. Fabian, S. Granade, Bench- and field-scale evaluation of chromium and cadmium extraction by electrokinetics, *J. Hazard. Mater.* 110 (2004) 53–62. <https://doi.org/10.1016/j.jhazmat.2004.02.036>.
- [2] S. Wiczorek, H. Weigand, M. Schmid, C. Marb, Electrokinetic remediation of an electroplating site: design and scale-up for an in-situ application in the unsaturated zone, *Electrokinet. Remediat. - EREM 2003*. 77 (2005) 203–215. <https://doi.org/10.1016/j.enggeo.2004.07.011>.
- [3] R. Iannelli, M. Masi, A. Ceccarini, M.B. Ostuni, R. Lageman, A. Muntoni, D. Spiga, A. Polettini, A. Marini, R. Pomi, Electrokinetic remediation of metal-polluted marine sediments: experimental investigation for plant design, 13th Int. Symp. *Electrokinet. Remediat.* 2014. 181 (2015) 146–159. <https://doi.org/10.1016/j.electacta.2015.04.093>.
- [4] R. López-Vizcaíno, V. Navarro, M.J. León, C. Risco, M.A. Rodrigo, C. Sáez, P. Cañizares, Scale-up on electrokinetic remediation: Engineering and technological parameters, *J. Hazard. Mater.* 315 (2016) 135–143. <https://doi.org/10.1016/j.jhazmat.2016.05.012>.
- [5] M. Villen-Guzman, J.M. Paz-Garcia, J.M. Rodriguez-Maroto, F. Garcia-Herruzo, G. Amaya-Santos, C. Gomez-Lahoz, C. Vereda-Alonso, Scaling-up the acid-enhanced electrokinetic remediation of a real contaminated soil, 13th Int. Symp. *Electrokinet. Remediat.* 2014. 181 (2015) 139–145. <https://doi.org/10.1016/j.electacta.2015.02.067>.
- [6] M. Masi, A. Ceccarini, R. Iannelli, Model-based optimization of field-scale electrokinetic treatment of dredged sediments, *Chem. Eng. J.* 328 (2017) 87–97. <https://doi.org/10.1016/j.cej.2017.07.004>.
- [7] Y.B. Acar, A.N. Alshawabkeh, Principles of electrokinetic remediation, *Environ. Sci. Technol.* 27 (1993) 2638–2647. <https://doi.org/10.1021/es00049a002>.
- [8] Acar Yalçın B., Alshawabkeh Akram N., Electrokinetic Remediation. I: Pilot-Scale Tests with Lead-Spiked Kaolinite, *J. Geotech. Eng.* 122 (1996) 173–185. [https://doi.org/10.1061/\(ASCE\)0733-9410\(1996\)122:3\(173\)](https://doi.org/10.1061/(ASCE)0733-9410(1996)122:3(173)).
- [9] K.R. Reddy, U.S. Parupudi, Removal of chromium, nickel and cadmium from clays by in-situ electrokinetic remediation, *J. Soil Contam.* 6 (1997) 391–407. <https://doi.org/10.1080/15320389709383574>.
- [10] K.R. Reddy, C. Chaparro, R.E. Saichek, Removal of Mercury from Clayey Soils Using Electrokinetics, *J. Environ. Sci. Health Part A*. 38 (2003) 307–338. <https://doi.org/10.1081/ESE-120016897>.
- [11] C. Cameselle, Effects of Periodic Electric Potential and Electrolyte Recirculation on Electrochemical Remediation of Contaminant Mixtures in Clayey Soils, *Water. Air. Soil Pollut. v.* 224 (2013) 1636–1636. <https://doi.org/10.1007/s11270-013-1636-8>.
- [12] F. Portet-Kotalo, M.T. Ammami, A. Benamar, H. Wang, F. Le Derf, C. Duclairoir-Poc, Investigation of the release of PAHs from artificially contaminated sediments using cyclolipopeptidic biosurfactants, *J. Hazard. Mater.* 261 (2013) 593–601. <https://doi.org/10.1016/j.jhazmat.2013.07.062>.
- [13] T. Suzuki, M. Moribe, Y. Okabe, M. Niinae, A mechanistic study of arsenate removal from artificially contaminated clay soils by electrokinetic remediation, *J. Hazard. Mater.* 254–255 (2013) 310–317. <https://doi.org/10.1016/j.jhazmat.2013.04.013>.
- [14] T. Suzuki, M. Niinae, T. Koga, T. Akita, M. Ohta, T. Choso, EDDS-enhanced electrokinetic remediation of heavy metal-contaminated clay soils under neutral pH conditions, 10th Int. Symp. *Electrokinet. Phenom.* 440 (2014) 145–150. <https://doi.org/10.1016/j.colsurfa.2012.09.050>.

- [15] C. Yuan, C.-H. Weng, Electrokinetic enhancement removal of heavy metals from industrial wastewater sludge, *Chemosphere*. 65 (2006) 88–96. <https://doi.org/10.1016/j.chemosphere.2006.02.050>.
- [16] A.Z. Al-Hamdan, K.R. Reddy, Transient behavior of heavy metals in soils during electrokinetic remediation, *Chemosphere*. 71 (2008) 860–871. <https://doi.org/10.1016/j.chemosphere.2007.11.028>.
- [17] S. Gan, E.V. Lau, H.K. Ng, Remediation of soils contaminated with polycyclic aromatic hydrocarbons (PAHs), *J. Hazard. Mater.* 172 (2009) 532–549. <https://doi.org/10.1016/j.jhazmat.2009.07.118>.
- [18] A. Colacicco, G. De Gioannis, A. Muntoni, E. Pettinao, A. Poletti, R. Pomi, Enhanced electrokinetic treatment of marine sediments contaminated by heavy metals and PAHs, *Chemosphere*. 81 (2010) 46–56. <https://doi.org/10.1016/j.chemosphere.2010.07.004>.
- [19] A. Benamar, F. Baraud, Electrokinetic remediation of dredged sediments from Le Havre Harbour, *Eur. J. Environ. Civ. Eng.* 15 (2011) 215–228. <https://doi.org/10.1080/19648189.2011.9693319>.
- [20] M.T. Ammami, A. Benamar, H. Wang, C. Bailleul, M. Legras, F. Le Derf, F. Portet-Koltalo, Simultaneous electrokinetic removal of polycyclic aromatic hydrocarbons and metals from a sediment using mixed enhancing agents, *Int. J. Environ. Sci. Technol.* 11 (2014) 1801–1816. <https://doi.org/10.1007/s13762-013-0395-9>.
- [21] J.N. Hahladakis, A. Latsos, E. Gidarakos, Performance of electroremediation in real contaminated sediments using a big cell, periodic voltage and innovative surfactants, *J. Hazard. Mater.* 320 (2016) 376–385. <https://doi.org/10.1016/j.jhazmat.2016.08.003>.
- [22] Y. Song, M.-T. Ammami, A. Benamar, S. Mezazigh, H. Wang, Effect of EDTA, EDDS, NTA and citric acid on electrokinetic remediation of As, Cd, Cr, Cu, Ni, Pb and Zn contaminated dredged marine sediment, *Environ. Sci. Pollut. Res.* 23 (2016) 10577–10586. <https://doi.org/10.1007/s11356-015-5966-5>.
- [23] M. Masi, A. Ceccarini, R. Iannelli, Multispecies reactive transport modelling of electrokinetic remediation of harbour sediments, *J. Hazard. Mater.* 326 (2017) 187–196. <https://doi.org/10.1016/j.jhazmat.2016.12.032>.
- [24] M. Villen-Guzman, C. Gomez-Lahoz, F. Garcia-Herruzo, C. Vereda-Alonso, J.M. Paz-Garcia, J.M. Rodriguez-Maroto, Specific Energy Requirements in Electrokinetic Remediation, *Transp. Porous Media.* 121 (2018) 585–595. <https://doi.org/10.1007/s11242-017-0965-2>.
- [25] Y. Song, A. Benamar, S. Mezazigh, H. Wang, Citric Acid-Enhanced Electroremediation of Toxic Metal-Contaminated Dredged Sediments: Effect of Open/Closed Orifice Condition, Electric Potential and Surfactant, *Pedosphere*. 28 (2018) 35–43. [https://doi.org/10.1016/S1002-0160\(18\)60003-7](https://doi.org/10.1016/S1002-0160(18)60003-7).
- [26] E. Kariminezhad, M. Elektorowicz, Comparison of constant, pulsed, incremental and decremental direct current applications on solid-liquid phase separation in oil sediments, *J. Hazard. Mater.* 358 (2018) 475–483. <https://doi.org/10.1016/j.jhazmat.2018.04.002>.
- [27] Y. Song, L. Cang, Y. Zuo, J. Yang, D. Zhou, T. Duan, R. Wang, EDTA-enhanced electrokinetic remediation of aged electroplating contaminated soil assisted by combining dual cation-exchange membranes and circulation methods, *Chemosphere*. 243 (2020) 125439. <https://doi.org/10.1016/j.chemosphere.2019.125439>.
- [28] R. López-Vizcaíno, J. Alonso, P. Cañizares, M.J. León, V. Navarro, M.A. Rodrigo, C. Sáez, Electroremediation of a natural soil polluted with phenanthrene in a pilot plant, *J. Hazard. Mater.* 265 (2014) 142–150. <https://doi.org/10.1016/j.jhazmat.2013.11.048>.
- [29] J.W. Schultze, M. Schweinsberg, From pm to km: scaling up and scaling down of electrochemical systems with TiO₂ and ZrO₂ passive films as an example,

- Electrochimica Acta. 43 (1998) 2761–2772. [https://doi.org/10.1016/S0013-4686\(98\)00017-6](https://doi.org/10.1016/S0013-4686(98)00017-6).
- [30] B.-K. Kim, K. Baek, S.-H. Ko, J.-W. Yang, Research and field experiences on electrokinetic remediation in South Korea, *Sci. Adv. Innov. Appl. Electrokinet. Remediat.* 79 (2011) 116–123. <https://doi.org/10.1016/j.seppur.2011.03.002>.
- [31] D.-H. Kim, S.-U. Jo, J.-C. Yoo, K. Baek, Ex situ pilot scale electrokinetic restoration of saline soil using pulsed current, *Sep. Purif. Technol.* 120 (2013) 282–288. <https://doi.org/10.1016/j.seppur.2013.10.007>.
- [32] S. Jorfi, S. Pourfadakari, M. Ahmadi, Electrokinetic treatment of high saline petrochemical wastewater: Evaluation and scale-up, *J. Environ. Manage.* 204 (2017) 221–229. <https://doi.org/10.1016/j.jenvman.2017.08.058>.
- [33] A. H. Sulaymon, Scale-Up of Electrochemical Reactors, in: A. H. Abbar ED1 - Vladimir Linkov ED2 - Janis Kleperis (Ed.), *Electrolysis*, IntechOpen, Rijeka, 2012: p. Ch. 9. <https://doi.org/10.5772/48728>.
- [34] A. Benamar, Y. Tian, F. Portet-Koltalo, M.T. Ammami, N. Giusti-Petrucciani, Y. Song, C. Boulangé-Lecomte, Enhanced electrokinetic remediation of multi-contaminated dredged sediments and induced effect on their toxicity, *Chemosphere.* 228 (2019) 744–755. <https://doi.org/10.1016/j.chemosphere.2019.04.063>.
- [35] Y. Tian, C. Boulangé-Lecomte, A. Benamar, N. Giusti-Petrucciani, A. Duflot, S. Olivier, C. Frederick, J. Forget-Leray, F. Portet-Koltalo, Application of a crustacean bioassay to evaluate a multi-contaminated (metal, PAH, PCB) harbor sediment before and after electrokinetic remediation using eco-friendly enhancing agents, *Sci. Total Environ.* 607–608 (2017) 944–953. <https://doi.org/10.1016/j.scitotenv.2017.07.094>.
- [36] M.T. Ammami, F. Portet-Koltalo, A. Benamar, C. Duclairoir-Poc, H. Wang, F. Le Derf, Application of biosurfactants and periodic voltage gradient for enhanced electrokinetic remediation of metals and PAHs in dredged marine sediments, *Chemosphere.* 125 (2015) 1–8. <https://doi.org/10.1016/j.chemosphere.2014.12.087>.